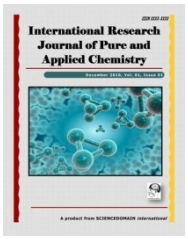

International Research Journal of Pure & Applied Chemistry
2(4): 286-304, 2012

SCIENCEDOMAIN *international*
www.sciencedomain.org

Adsorption and Inhibitive Effects of 2-Thiobenzylbenzimidazole (TBBI) at Aluminium Alloy AA3003/ 1M Hydrochloric Acid Interface

P. M. Niamien[1*], A. A. Koffi[1] and A. Trokourey[1]

[1]Laboratoire de chimie physique. Université de Cocody-Abidjan.

Authors' contributions

This work was carried out in collaboration between all authors. Author PMN designed the study, performed the statistical analysis, wrote the protocol and wrote the first draft of the manuscript. Author AAK managed the analyses of the study. Author AT managed the literature searches. All authors read and approved the final manuscript.

Research Article

Received 1st August 2012
Accepted 5th November 2012
Published 6th December 2012

ABSTRACT

The interfacial behavior of 2-Thiobenzylbenzimidazole (TBBI) between aluminium alloy AA 3003 and 1M hydrochloric acid solution was investigated by mass loss technique. Mass loss is concentration and temperature dependent. The influence of temperature has been studied in the absence and in presence of TBBI in the hydrochloric solution in the range 35-55ºC. Adsorption isotherms models including Langmuir, Temkin, Freundlich and El-Awady were tested. It was found that the inhibitor adsorbs on the metal according to the modified Langmuir adsorption isotherm. Some thermodynamic adsorption parameters (ΔG°_{ads} ΔH°_{ads}, ΔS°_{ads}) as well as activation parameters including apparent activation energy (E_a), change in activation enthalpy (ΔH^{*}_{a}) and change in activation entropy (ΔS^{*}_{a}) have been calculated and analyzed. Furthermore the Dubinin-Raduskevitch model has been used to distinguish between chemisorption and physisorption. The properties most relevant to the potential action as a corrosion inhibitor of TBBI have been calculated: highest occupied molecular orbital energy (E_{HOMO}), lowest unoccupied molecular orbital energy (E_{LUMO}), energy gap (ΔE), dipole moment (μ) and charges on the adsorption centers (S, N) and C atoms in benzimidazole and benzyl rings. These calculations were performed using the Gaussian

**Corresponding author: Email: niamienfr@yahoo.fr;*

suite of programs level by DFT/B3LYP/6-31G (d,p). The theoretical results are consistent with the experimental data.

Keywords: Interfacial behavior; corrosion inhibitor; adsorption isotherm; standard free adsorption energy; activation energy; quantum calculations.

1. INTRODUCTION

Aluminium and its alloys are important materials with a wide range of industrial applications because of their appearance, low density, corrosion resistance and their low cost [1-4]. The corrosion resistance of aluminium and its alloys arises from their ability to form a natural oxide film on their surfaces in a variety of media. Because of this advantage, aluminium and its alloys are widely used in many industries such as machinery and heat exchanger industries; acids are normally used for industrial cleaning, process that leads to substantial loss of material. In contact with acids such as hydrochloric acid, sulfuric acid, nitric acid, the oxide film is susceptible to corrosion [5,6]. Several authors [7,8] have studied the corrosion of aluminium and its alloys and their corrosion inhibition by organic inhibitors in acidic solutions. Usually, organic compounds are widely used in industry for preventing corrosion in acidic environments [9-12].

Corrosion inhibitors are chemical compounds used in small concentrations whenever a metal is in contact with an aggressive medium. The presence of such compounds retards the corrosion process and keeps its rate to a minimum and thus prevents economic losses due to metal corrosion. The inhibitive power of the organic inhibitors has been interpreted in term of many different characteristics such as molecular size, molecular weight, molecular structure, nature of heteroatom present in the molecule [2,3]. Organic compounds, containing electronegative functional groups and π-electrons in triple or conjugated double bonds, are usually good inhibitors. Heteroatoms as sulphur, phosphorus, nitrogen and oxygen as well as aromatic rings in their structures are major adsorption centers. The inhibition efficiency has found to be closely related to inhibitor adsorption abilities due to the presence of heteroatoms (O, N, S, P…). Generally, the tendency to form a stronger coordination bond and consequently resulting in high inhibition efficiency increases in the following order: O < N < S < P [13]. It has been assumed that the first stage in the action mechanism of the inhibitors in aggressive acidic media is the adsorption onto the metal surface. The processes of adsorption of inhibitors are influenced by the nature and the surface charge of the metal, the chemical structure of organic compounds, the distribution of charge in the molecule, the type of aggressive electrolyte and type of interaction between the organic molecules and the metallic surface [14-16]. Physical adsorption and chemisorption are the principal type of interaction between the organic inhibitor and the metal surface [16]. Various aliphatic and aromatic amines as well as nitrogen heterocyclic compounds have been tested as corrosion inhibitors for pure aluminium in acid media [17-19]. Hydrazine compounds [20-22], organic acids and their salts [23] were also found to inhibit the corrosion of aluminium in hydrochloric acid solutions.

This work is devoted to the study of 2- thiobenzylbenzimidazole (TBBI) as a corrosion inhibitor of aluminium alloy AA 3003 in 1M hydrochloric acid solution. The aluminium alloy AA 3003 is used in heat exchanger industry, particularly as heater core. The choice of this compound was based on the consideration that this molecule contains two nitrogen atoms, one sulphur atom, π-electrons in the benzimidazole and the benzyl rings. A survey of

literature has shown that no work has yet been done on this molecule in contact with this interface (Aluminium alloy AA 3003/ hydrochloric acid).

2. MATERIALS AND METHODS

2.1 Aluminium Alloy

Our samples were rods of aluminium alloy (AA 3003) measuring 1.2 cm in length and 0.3 cm in diameter. The composition of our sample is: Mn-1.32% Fe-0.45% Cu-0.11% Si-0.23% Mg-0.02% Cr-0.01% Zn-0.01% and the remainder being Al.

2.2 Solutions

The aggressive solutions used were made of analytical reagent grade hydrochloric acid from Merck. The 1M hydrochloric acid solution was prepared using double distilled water. The concentration range of TBBI employed was 5.10^{-5} to 10^{-3} M in 1M hydrochloric acid.

2.3 Mass Loss Measurement

The mass loss method of monitoring corrosion rate is useful because of its simple application and reliability [24]. Several authors have reported on a comparable agreement between mass loss technique and other techniques of corrosion monitoring including polarization measurement [25-27], hydrogen evolution [28-31], Thermometric technique [32,33] and electrochemical impedance spectroscopy [34,35].

The samples were polished successively with fine grade emery papers, cleaned with acetone, washed with double distilled water and dried in moisture free desiccator. Tests were conducted under total immersion conditions in 50 mL of test solutions maintained at (35-55ºC). The pre-cleaned and weighed samples were in the beaker containing the test solution: all tests were made in aerated solutions and were run triplicate to guarantee the reliability of the results. To determine the mass loss at the end of the test, the samples were retrieved from test solutions after 1 hour, washed with bi-distilled water, dried, kept in a desiccator and then reweighed. The mass loss was taken as the difference between the initial mass and the mass after 1 hour immersion time. The corrosion rate (W) was calculated according to equation (1):

$$w = \frac{m_1 - m_2}{S\,t} \quad (1)$$

where m_1 and m_2 are respectively the mass (in g) before and after immersion in the test solution, S is the total surface of the sample (in cm^2) and t is the immersion time (in h). The inhibition efficiency IE (%) was then calculated using the relation (2):

$$IE(\%) = \frac{W_0 - W}{W_0} * 100 \quad (2)$$

w_0 and w are respectively the corrosion rates of aluminium alloy AA 3003 in the absence and presence of the tested compounds.

2.4 Structure of TBBI

The structure of the organic compound used as inhibitor is given in Fig.1.

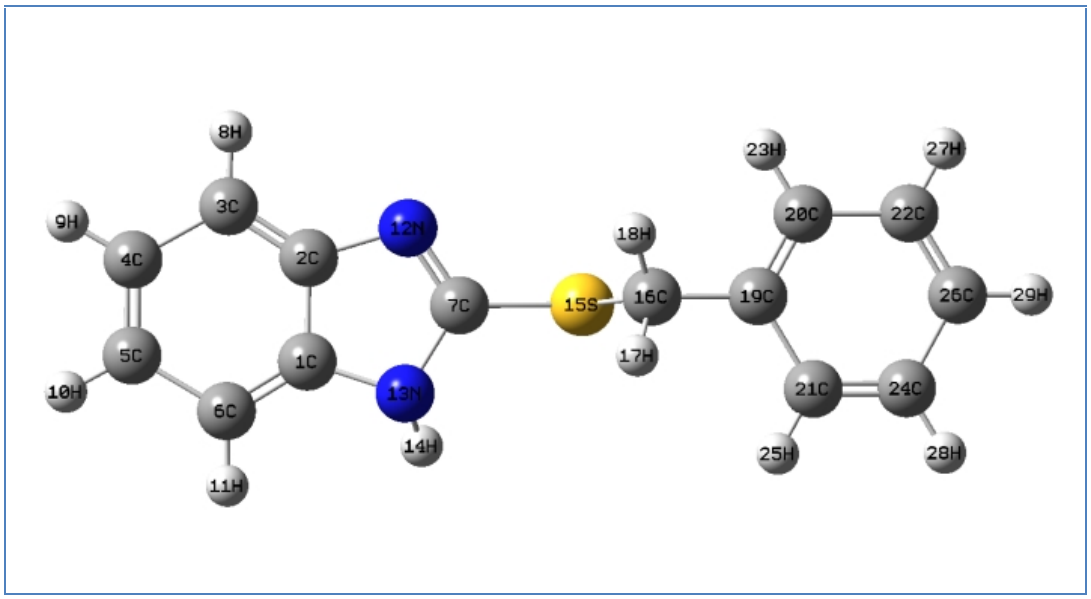

Fig. 1. Optimized structure of 2-thiobenzylbenzimidazole (TBBI)

This organic compound has been synthesized in the laboratory. Its molecular structure has been identified by ^{1}H NMR and ^{13}C spectroscopies and mass spectroscopy.

^{1}H NMR (DMSO-d_6) 4.57 (C$\underline{H}_2$, 2H, s), 7.10-7.16 (2H_{ar},m), 7.22-734 (3H_{ar},m), 7.44 (2H_{ar},m), 7.46-7.47(2H_{ar},m) ^{13}C NMR (50MHz, DMSOd-6) 35.12 ($\underline{C}H_2$), 114.08 (2C_{ar}) , 121.39 (2C_{ar}), 127.27 (C_{ar}), 128.44 (2C_{ar}), 128.80 (2C_{ar}), 137.64 (C_{ar}), 150 (C=N); SDM (E.I.) : M^{+1} = 241. Analysis for $C_{14}H_{12}N_2S$: C(69.97%), H(5.03%), N(11.66%), S(13.34%).

3. RESULTS AND DISCUSSION

3.1 Corrosion Rate and Inhibition Efficiency

Fig. 2 shows the evolution of mass loss with concentration in the absence and presence of TBBI at different temperatures. It is clear that the corrosion rate of the aluminium alloy decreases in presence of TBBI when compared to the Blank. The obtained curves at different temperatures fall with increasing concentration of TBBI. These results indicate that TBBI in the HCl solution inhibits the corrosion of aluminium and the extent of corrosion inhibition depends on the amount of TBBI present. The curves also indicate that the mass loss of aluminium alloy AA 3003 increases with increasing temperature at all concentration of TBBI. This can be explained by an increase in chemical reaction when the temperature increases. Corrosion of aluminium in aqueous acid solution has been reported [36] to depend on the concentration of anion in solution.

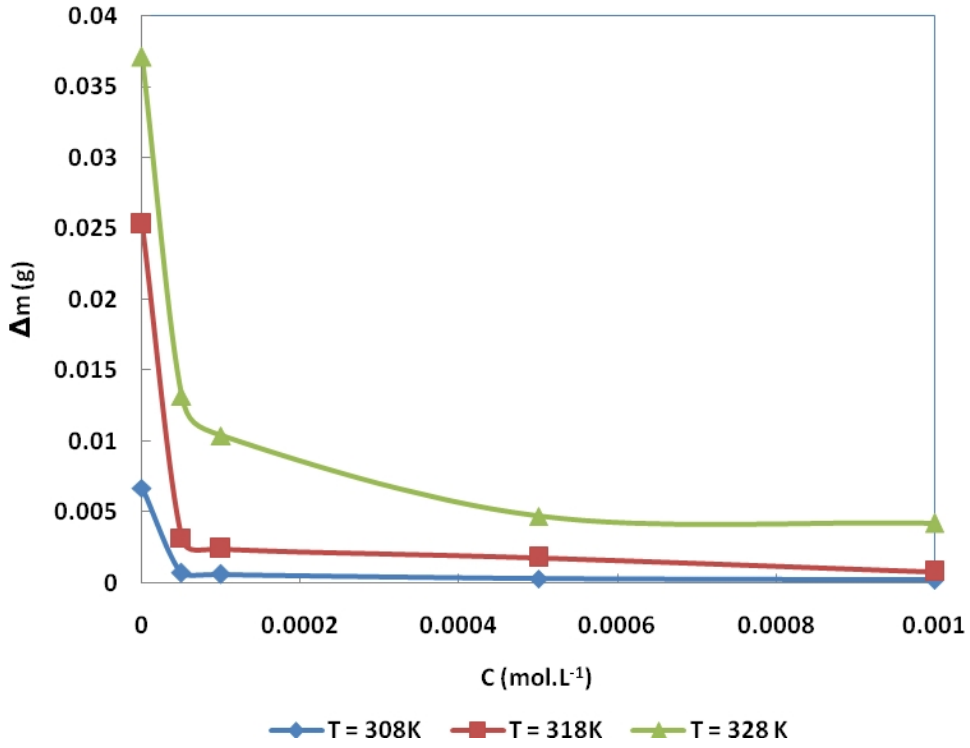

Fig. 2. Dependence of mass loss on concentration of TBBI at different temperatures in the immersion period of 1h in 1.0 M HCl

Each Δm value is expressed as mean ± 0.0002g.

A general mechanism [36] for the dissolution of aluminium would be similar to that reported:

$$Al_{(s)} + H_2O \rightleftarrows AlOH_{ads} + H^+ + e^- \quad \text{(a)}$$

$$AlOH_{ads} + 5H_2O + H^+ \rightleftarrows Al^{3+}.6H_2O + 2e^- \quad \text{(b)}$$

$$Al^{3+} + H_2O \rightleftarrows [AlOH]^{2+} + H^+ \quad \text{(c)}$$

$$[AlOH]^{2+} + X^- \rightleftarrows [AlOHX]^+ \quad \text{(d)}$$

The controlling step in the metal dissolution is the complexation reaction between the hydrated cation and the anion present (Eq. (d)). In the presence of chloride ions the reaction will be:

$$[AlOH]^{2+} + Cl^- \rightleftarrows [AlOHCl]^+$$

The soluble complex ion formed increases the metal dissolution rate which depends on the chloride concentration; this can explain the increase in corrosion rate in HCl (Blank) as compared to the presence of TBBI where the contact between the chloride ions and the hydrated cation is avoided.

The values of inhibition efficiency obtained from mass loss method at different concentrations of TBBI and at different temperatures in 1M hydrochloric acid solution are shown in Fig. 3.

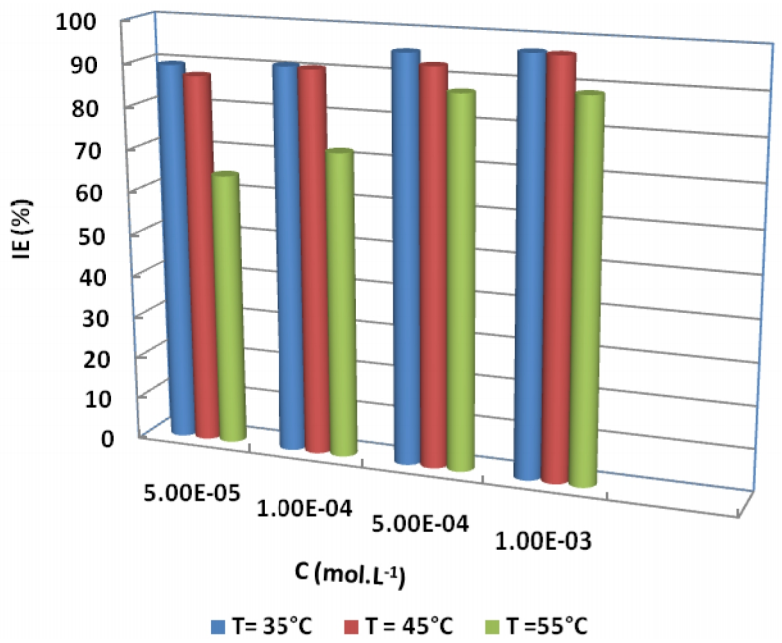

Fig. 3. Dependence of inhibition efficiency on concentration of TBBI at different temperatures in 1.0 M HCl

Each IE value is expressed as mean ± 0.2(%).

Inhibition efficiency is concentration and temperature dependent: the inhibition efficiency increases with increasing concentration but decreases with increase in temperature. It is seen that the inhibition efficiency reaches a maximum value of 97% at 35ºC and a value of 88,7% at 55ºC, at C = 10^{-3}M. The inhibition efficiency decreases, with increasing temperature; that is suggestive of physical adsorption mechanism and may be attributed to increase in the solubility of the protective barrier formed and of any reaction product precipitated on the surface of the metal that otherwise inhibit the corrosion process. The decrease of inhibition efficiency with increase in temperature could also be attributed to a possible shift of the adsorption-desorption equilibrium towards desorption of the adsorbed inhibitor molecules due to increased solution agitation.

3.2 Adsorption Isotherm

The adsorption of an organic inhibitor on the surface of a corroding metal may be regarded as a substitution process between the organic compound in aqueous phase and water molecules adsorbed on the metal surface [37]:

$$Org_{sol} + xH_2O_{ads} \leftrightarrow Org_{ads} + xH_2O_{sol}$$

where *Org* $_{(sol)}$ and *Org* $_{(ads)}$ are respectively the organic species dissolved in the aqueous solution and adsorbed onto the metallic surface; H_2O $_{(ads)}$ and H_2O $_{(sol)}$ are the water molecule adsorbed onto the metallic surface and that in the bulk solution; *x* is the size ratio representing the number of water molecules replaced by one organic adsorbate. The surface coverage (θ) was calculated from mass loss, using Eq. 3.

$$\theta = \frac{W_0 - W}{W_0} \quad (3)$$

Basic information on the interaction between the inhibitor and the aluminium surface can be provided by the adsorption isotherm. In order to obtain the adsorption isotherm, a linear relation between θ values and inhibitor concentration C must be found. Attempts were made to fit the θ values to various isotherms including Langmuir, Temkin, Freundlich and El-Awady kinetic/thermodynamic model. Tested isotherms are shown in Table 1.

Table 1. Equations of the tested adsorption isotherms

Isotherm	Equation
Langmuir	$\frac{C_{inh}}{\theta} = \frac{1}{K_{ads}} + C_{inh}$
Temkin	$\theta = \frac{2.303}{f}[logK_{ads} + logC_{inh}]$
Freundlich	$log\theta = logK_{ads} + n\ logC_{inh}$
El-Awady	$log\left(\frac{\theta}{1-\theta}\right) = \log K \ + y\ logC_{inh}$

Fig. 4 shows the plots of the studied isotherms. They all yield straight lines. The parameters of these isotherms are listed in Table 2.

Table 2. The isotherms parameters for various temperatures

Isotherm	T(K)	R^2	Slope	Intercept
Langmuir	308	0.999	1.025	$7.051\ 10^{-6}$
	318	0.999	1.029	$1.075\ 10^{-5}$
	328	0.999	1.104	$2.450\ 10^{-5}$
Temkin	308	0.995	0.060	1.150
	318	0.936	0.064	1.153
	328	0.972	0.194	1.489
Freundlich	308	0.997	0.028	0.703
	318	0.938	0.029	0.712
	328	0.966	0.109	0.289
El- Awady	308	0.983	0.454	2.854
	318	0.864	0.424	2.657
	328	0.982	0.516	2.486

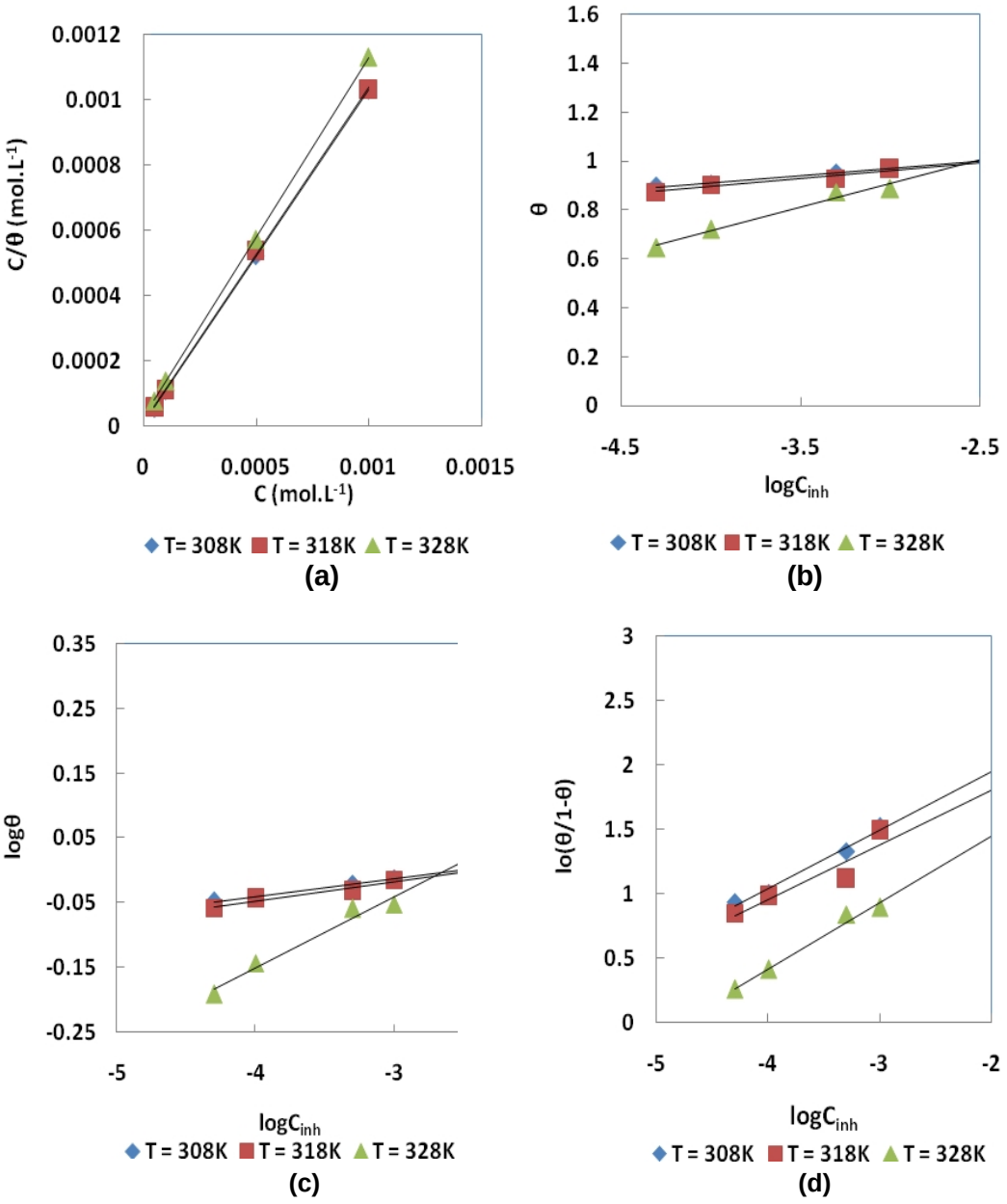

Fig. 4. Adsorption isotherms for TBBI at different temperatures in 1.0 M HCl. (a) Langmuir isotherm, (b) Temkin isotherm,(c) Freundlich isotherm, (d) El - Awady isotherm

Correlation coefficient (R^2) values were used to determine the best fit isotherm. By far the best fit for the experimental data was obtained with the Langmuir isotherm. The values of the correlation coefficients and that of the slopes of the straight lines in the case of this isotherm are all very close to one. However, we can observe a deviation of the slopes from unity; this is often interpreted as a sign that the adsorbed species occupy more or less a

typical adsorption site at the metal/solution interface [38]. The deviation from unity is also attributable to interactions between adsorbate species on the metal as well as changes in the adsorption heat with increasing surface coverage [36]; these factors were not taken into consideration in the derivation of Langmuir isotherm. Examining Table 2, one can see that according to El- Awady's isotherm one molecule of TBBI replaces two molecules of water (1/y = 2); the slopes of The Temkin isotherm shows repulsive interactions between TBBI molecules and that of Freundlich isotherm indicates a heterogeneity character of the surface 0 < n < 1. So, Langmuir adsorption isotherm cannot be applied rigorously. The adsorption behavior of TBBI is more appropriate to the modified Langmuir adsorption isotherm [39] which is characterized by Eq. (4).

$$\frac{C}{\theta} = \frac{n}{K_{ads}} + nc \tag{4}$$

where C is the inhibitor concentration, θ is the fraction of the surface covered and K_{ads} is the equilibrium constant of the adsorption process.

Free adsorption energy ΔG^0_{ads} was then calculated using Eq. (5):

$$K_{ads} = \frac{1}{55.5} \exp\left(-\frac{\Delta G^0_{ads}}{RT}\right) \tag{5}$$

55.5 is the molar concentration of water in the solution in $mol.L^{-1}$. The obtained values of equilibrium constant and free adsorption energy at different temperatures are summarized in Table 3.

The negative values of ΔG^0_{ads} indicates a spontaneous adsorption of the molecules on the aluminium alloy surface. According to several authors [40,41], it is accepted that for the values of ΔG^0_{ads} up to - 20 $kJmol^{-1}$ the type of adsorption is physisorption while the values more negative than - 40 kJ mol^{-1} lead to chemisorption. In our case, the values of ΔG^0_{ads} are around - 40 kJ mol^{-1}: it is suggested that the adsorption of TBBI involves both physisorption and chemisorption. The relation between ΔG^0_{ads}, ΔH°_{ads} and ΔS°_{ads} is given by the following basic equation:

$$\Delta G^\circ_{ads} = \Delta H^\circ_{ads} - T\Delta S^\circ_{ads} \tag{6}$$

Change in enthalpy ΔH°_{ads} and change in entropy ΔS°_{ads} of the adsorption process can be obtained by plotting ΔG^0_{ads} versus temperature (Fig. 5). The straight line obtained has a slope equals to ($-\Delta S^\circ_{ads}$) and an intercept equals to (ΔH°_{ads}). The values of these parameters are also listed in Table 3.

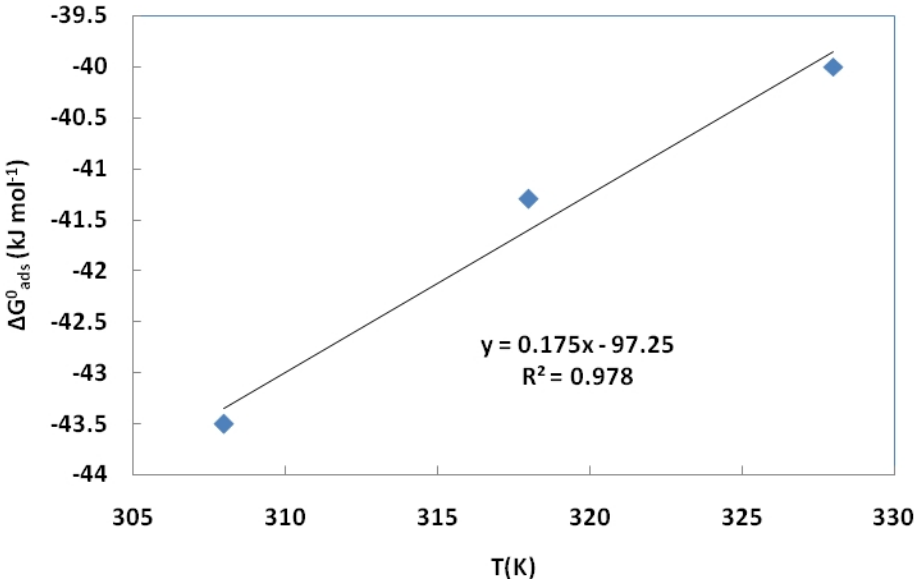

Fig. 5. ΔG^0_{ads} versus temperature for aluminium alloy AA 3003 in HCl 1.0 M

Table 3. Langmuir isotherm parameters at different temperatures

Temperature (K)	K_{ads} (10^5 M^{-1})	$\Delta G°_{ads}$ (kJ mol^{-1})	ΔH°_{ads} (kJ mol^{-1})	$-\Delta S^{\circ}_{ads}$ (J $mol^{-1}K^{-1}$)
308	2.56	- 43.5	- 95.25	175
318	1.97	- 41.3	-	-
328	0.43	- 40.0	-	-

3.3 Activation Energy

To elucidate the mechanism of inhibition process, the apparent activation energy (E_a) in the absence and that in the presence of the inhibitor were evaluated using a modified form of the Arrhenius equation [42]:

$$logW = logk - \frac{E_a}{2,3RT} \quad (7)$$

E_a is the apparent activation energy, k is the preexponential factor, R is the molar gas constant and T is the absolute temperature. Plotting logW versus 1/T (Fig. 6) for the blank and the solution containing the inhibitor leads to E_a values (Table 4).

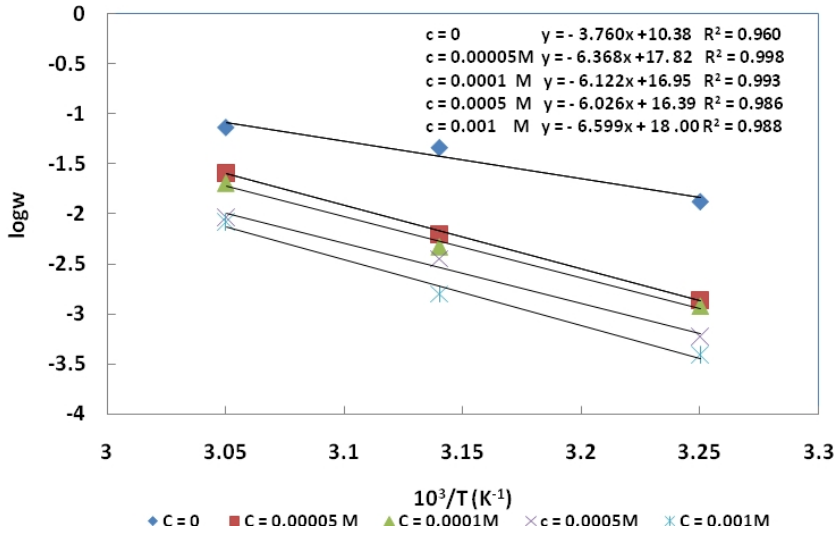

Fig. 6. Arrhenius plots for blank and solutions containing various concentrations of TBBI

The thermodynamic activation parameters including change in enthalpy (ΔH_a^*) and change in entropy (ΔS_a^*) of activation were calculated using the transition state equation [36]:

$$log\left(\frac{W}{T}\right) = \left[log\left(\frac{R}{Nh}\right) + \left(\frac{\Delta S_a^*}{2.303R}\right)\right] - \frac{\Delta H_a^*}{2.303RT} \quad (8)$$

where k_B is the Boltzmann constant (1.3810^{-23} J K^{-1}), h is the Planck constant ($6.626\ 10^{-34}$ J s), R is the perfect gas constant and N is the Avogadro number. Fig. 7 shows a plot of log (W/T) versus 1/T.

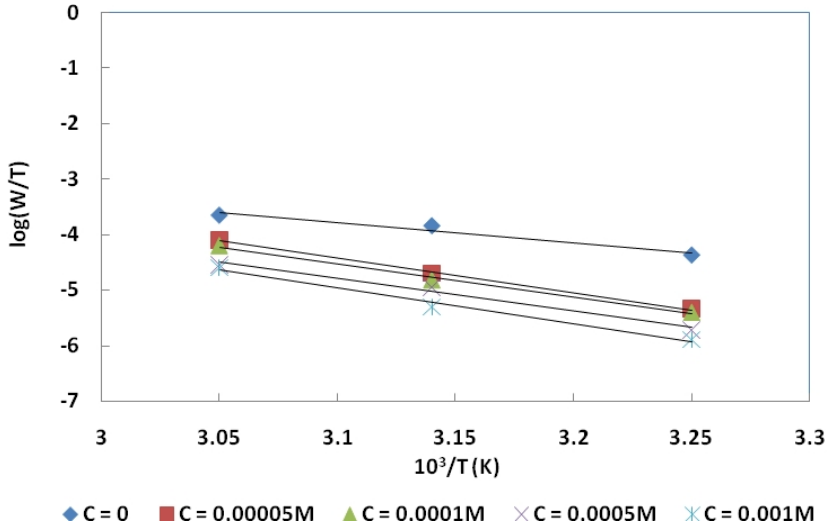

Fig. 7. Arrhenius plots of $log\left(\frac{W}{T}\right)$ versus $\frac{1}{T}$ at different concentration of TBBI

Straight lines are obtained with a slope of $\left(-\frac{\Delta H_a^*}{2.303R}\right)$ and from the intercepts of $log\left(\frac{W}{T}\right)$ – axis, ΔS_a^* values were calculated. All the thermodynamic activation parameters are given in Table 4.

The relationship between the temperature dependence of inhibition efficiency IE (%) of an inhibitor and the apparent activation energy found in its presence is given as follows [43]:

- ✓ Inhibitors whose IE (%) decreases with increasing temperature. The value of apparent activation energy is greater than that in the uninhibited solution.
- ✓ Inhibitors whose IE (%) does not change with temperature variation. The apparent activation energy (E_a) does not change with the presence or absence of the inhibitor;
- ✓ Inhibitors whose IE (%) increases with increase in temperature. The value of the activation energy (E_a) is less than that in the uninhibited solution.

Table 4. Activation parameters at various concentrations.

Concentration (M)	E_a (kJ mol^{-1})	ΔH_a^* (kJ mol^{-1})	ΔS_a^* (J mol K^{-1})
0	71.9	61.7	- 48.4
5.10^{-5}	121.7	119.3	87.6
10^{-4}	117.2	114.6	71.1
5.10^{-4}	115.2	112.7	60.2
10^{-3}	126.1	123.7	97.1

According to [44], the higher value of apparent activation energy of the process in the presence of an inhibitor when compared to that in its absence is attributed to its physical adsorption, its chemisorption is pronounced in the opposite case. In our case, the higher value of apparent activation energy in the presence of TBBI compared to that in its absence and the decrease of IE (%) with an increase in temperature can be interpreted as an indication of the existence of physical adsorption.

From Table 4, it can be seen that the values of activation energy E_a for the inhibited solutions are upper than that for the uninhibited one, indicating that physisorption is favored. The positive sign of change in activation enthalpy reflects the endothermic nature of the aluminium alloy dissolution process; the value of this parameter increases with increasing concentration of TBBI, indicating that the dissolution of the alloy becomes more and more difficult. The positive sign of change in entropy in the presence of the inhibitor indicates that disorder is increased on going from reactants to activated complex.

3.4 Adsorption Mechanism

To distinguish between physical and chemical adsorption, the experimental results obtained in this study were further fitted into Dubinin-Radushkevich isotherm model. Recently, this model has been applied [45] in explaining the mechanism of adsorption of corrosion inhibitor onto the aluminium surface in alkaline solutions. The equation of this model can be expressed as:

$$\ln \theta = \ln \theta_{max} - a\delta^2 \quad (9)$$

where θ_{max} is the maximum surface coverage and δ the Polanyi potential which can be expressed as:

$$\delta = RTln\left(1 + \frac{1}{C_{inh}}\right) \quad (10)$$

R is the universal gas constant, T is the absolute temperature and C_{inh} is the concentration of the inhibitor. The constant a gives the mean adsorption energy, E, which is the transfer energy of one mole of adsorbate from infinity (bulk solution) to the surface of adsorbent. E is given by the following equation:

$$E = \frac{1}{\sqrt{2a}} \quad (11)$$

The magnitude of E gives information about the type of adsorption. Values of E less than 8 kJ/mol indicates physical adsorption [45]. Plotting lnθ versus δ^2 leads to the mean adsorption energy via the value of the slope of the straight line (Fig. 8).

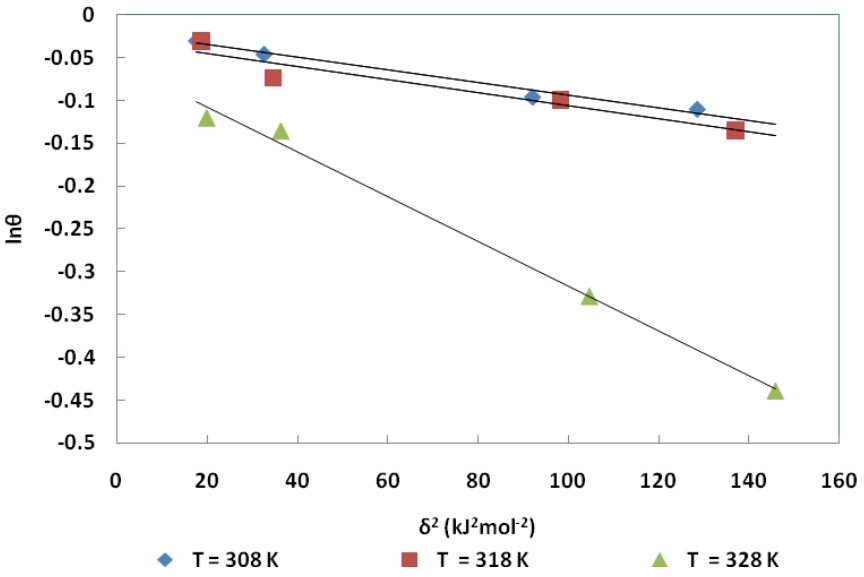

Fig. 8. Dubinin-Radushkevich plots for the adsorption of 2-Thiobenzylbenzimidazole on aluminium alloy AA3003 in 1M HCl

The parameters of the straight lines are listed in Table 5.

Table 5. Dubinin-Raduskevich isotherm parameters for the adsorption of TBBI on aluminium alloy AA3003 in 1M HCl

Temperature (K)	Equation	Correlation coefficient (R^2)	E (kJ mol^{-1})
308	$ln\theta = -0.0007\ \delta^2 - 0.0204$	0.978	26.7
318	$ln\theta = -0.0008\ \delta^2 - 0.0303$	0.912	25.0
328	$ln\theta = -0.0026\ \delta^2 - 0.0549$	0.995	13.9

Examining Table 5, one can see that the value of the mean adsorption energy decreases with increasing temperature, confirming the evolution of the inhibition efficiency when the temperature increases.

To gain insight into the relation between the type of adsorption and the temperature we have plotted E versus T (Fig. 9). The data give a straight line which equation allows determining the domain of temperatures corresponding to chemisorption and that of physisorption.

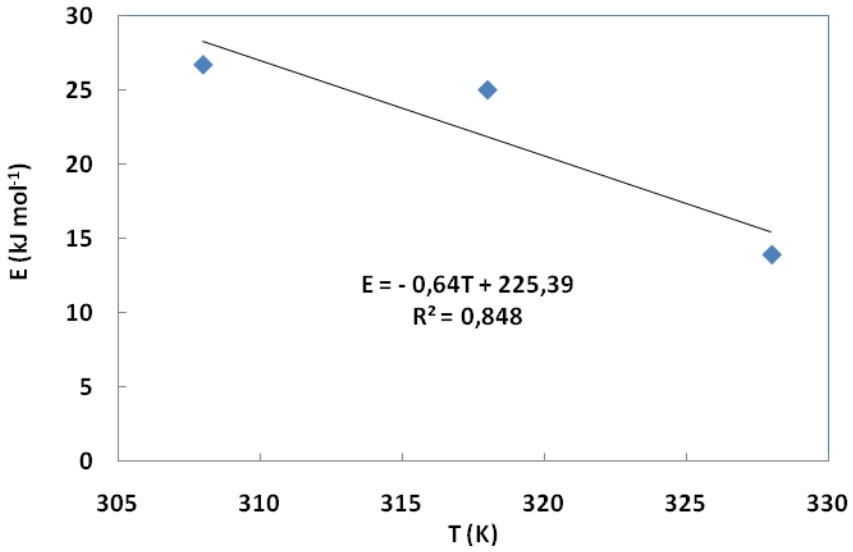

Fig. 9. Plot of mean energy versus temperature

The equation of the line $E = -0.64T + 225.39$ shows that:

- chemisorption is predominant for T < 339.7 K.
- physisorption is predominant for T > 339.7 K.

One can see that for the studied temperatures (35 - 55ºC); chemisorption plays the significant role in the adsorption of TBBI on the aluminium alloy AA 3003 in 1M HCl.

3.5 Corrosion Inhibition Mechanism

It is well known that chloride ions have a small degree of hydration, that they could bring excess negative charges in the vicinity of the interface and then, positively charged might adsorb onto the surface. TBBI might be protonated in the acid solution as follows:

$$TBBI + xH^{+} \leftrightarrow [TBBIH_x]^{x+}$$

The protonated TBBI, however, could attach to the aluminium alloy AA 3003 by means of electrostatic interactions between Cl^- and protonated TBBI. The schematic illustration of synergistic inhibition between chloride ions and protonated TBBI for the corrosion of aluminium alloy (AA 3003) in hydrochloric acid is presented in Fig. 10. Since aluminium alloy AA 3003 surface has positive charges in 1M HCl solution [46], obtained results could be

explained on the assumption that in the presence of chloride ions, the negatively charged Cl^- would attach to the positively charged surface [47]. There may be a synergism between Cl^- and protonated inhibitor. Near the interface, the concentrations of Cl^- and that of the protonated TBBI were probably much higher than those in the bulk solution, the protonated TBBI did attach directly to the negative charges on the aluminium alloy surface. When TBBI adsorbs on the Aluminium alloy surface, coordinate bonds are formed by partial transference of electrons from the unprotonated nitrogen atoms, sulphur atoms, delocalized π electrons in the benzimidazole and the benzyl rings to the metal surface. So, in the process of adsorption both physical and chemical adsorptions might take place. Similar mechanism has been proposed [48] in the literature.

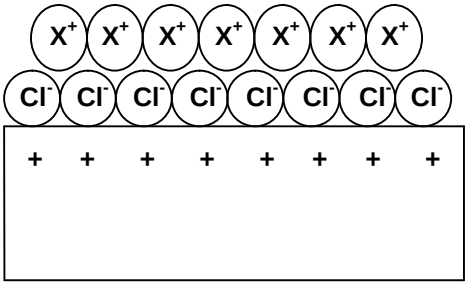

Fig. 10. Schematic illustration of synergetic inhibition between chloride ion and protaned TBBI ($[TBBIH_x]^{x+} = X^+$) for aluminium alloy AA 3003 in 1M HCl

3.6 Quantum Chemical Calculations

To investigate the effect of molecular structure on the inhibition mechanism and inhibition efficiency, some quantum chemical calculations were performed. Quantum chemical parameters such as the energy of highest occupied molecular orbital, E_{HOMO}, the energy of the lowest unoccupied molecular orbital E_{LUMO}, dipole moment μ of the molecule and charge densities on N, S atoms (adsorption centers) and around the C atoms of the benzimidazole and benzyl rings in the molecule have been calculated. These parameters were calculated using the Gaussian 03 W suite of programs. The calculations were performed using DFT/B3LYP/6-31G (d,p). The obtained parameters are listed in Tables 6 and 7.

Table 6. Quantum chemical parameters for TBBI

Parameters	M (g mol^{-1})	μ (Debye)	E_{HOMO} (eV)	E_{LUMO} (eV)	$\Delta E = E_{LUMO} - E_{HOMO}$ (eV)
Calculated value	240.07	1.878	- 5.606	- 0.484	5.122

Table 6 shows that TBBI has a relatively higher value of HOMO energy and a lower value of LUMO energy, which was in favor of bonding with metal surface, compared with some other organic heterocyclic inhibitors [49]. As E_{HOMO} is often associated with the electron donating ability of the molecule, high values of E_{HOMO} indicate a tendency of the molecule to donate electrons to appropriate acceptor molecule with low energy and empty molecular orbital. In our case, the electronic configuration of aluminium is $1S^2 2S^2 2P^6 3S^2 3P^1$; the incompletely filled 3P orbital could bond with HOMO of TBBI while the filled 3S orbital could interact with the LUMO of TBBI.

From Table 7, it can be seen that the negative charges are concentrated on the N and S atoms. In HCl solutions some of the N atoms are protonated, so the TBBI molecule could attach to the negatively charged surface of the metal due to the adsorption of Cl^- ions. The unprotonated N atoms and S atoms could then interact with the metal. The negative charges on some C atoms (4 C, 5 C) of benzimidazole ring and (20C, 21C, 22C, 24C and 26C) of benzyl ring also interact with aluminium alloy AA 3003. It can be seen from quantum parameters that the adsorption of TBBI could involve both physisorption and chemisorption.

Table 7. Charge density of atoms in the molecule of TBBI responsible for the interactions with the metal

N°	Atom	charge/e
4	C	- 0.096003
5	C	- 0.078984
12	N	- 0.674025
13	N	- 0.581071
15	S	- 0.354045
20	C	- 0.047205
21	C	- 0.047670
22	C	- 0.010848
24	C	- 0.010521
26	C	- 0.026008

4. CONCLUSION

From the experimental results the following conclusion can be deduced:

- 2-Thiobenzylbenzimidazole is a suitable inhibitor for aluminium alloy AA 3003 in 1M HCl; the inhibition efficiency increases with increasing concentration in TBBI but decreases with increase in temperature.
- TBBI adsorbs on aluminium alloy AA 3003 according to the modified Langmuir adsorption isotherm model.
- According to the kinetic/thermodynamic adsorption model of El-Awady, one molecule of TBBI replaces two molecules of water.
- The isotherms of Temkin and Freundlich show repulsive interactions between TBBI molecules.
- The values of ΔG°_{ads} and ΔH°_{ads} for all the studied temperatures show that TBBI is absorbed by a spontaneous exothermic process.
- Both physisorption and chemisorption are suggested from ΔG°_{ads} and the Dubinin-Radushkevich isotherm.
- Quantum chemical parameters support the experimental results.

ACKNOWLEDGMENTS

The authors gratefully acknowledged the support of the Physical Chemistry Laboratory of University of Abidjan-Cocody.

COMPETING INTERESTS

Authors have declared that no competing interests exist.

REFERENCES

1. Wen-Ta T, Yen-Huei H, Ju-Tung L. Corrosion inhibition of aluminium alloys in heat exchanger systems. Surf. Coat. Technol. 1987;31(4):365-379.
2. Muralidharan S, Quraishi MA, Lyer SVK. The effect of molecular structure on hydrogen permeation and the corrosion inhibition of mild steel in acidic solutions. Corros. Sci. 1995;37(11):1739-1750.
3. Quraishi MA, Khan MA, Wajid MA, Ajmal M, Muralidharan S, lyer S, Venkatakrishna S. Influence of molecular structure of substituted benzothiazoles on corrosion inhibition and hydrogen permeation through mild steel in sulphuric acid. Br. Corros. J. 1997;32(1):72-76.
4. Bazzi L, Salghi R, Ei Alami Z, Ait Addi E, El Issami S, Kertit S, Hammouti B. Comparative study of the effect of inorganic ions on the corrosion of Al 3003 and 6063 in carbonate solution. Prog. Org. Coat. 2004;51(2):113-117.
5. Ovari F, Tomcsanyi L, Turmezey T. Electrochemical study of the pitting corrosion of aluminium and its alloys-I. Determination of critical pitting and protection potential. Electrochim. Acta. 1988;33(3):323-326.
6. Tomcsanyi L, Varga K, Bartk I, Horanyi G, Malezki E. Electrochemical study of the pitting corrosion of aluminium and its alloys- II. Study of interaction of chloride ions with a passive film on aluminium and initiation of pitting corrosion. Electrochim. Acta. 1989;34(6):855-859.
7. Stevanovic RM, Despic AR, Drazic DM. Activation of aluminium in chloride containing solutions. Electrochim. Acta. 1988;33(3):397- 404.
8. Frers SE, Stefenal MM, Mayer C, Chierchie T J. AC - Impedance measurements on aluminium in chloride containing solutions and below the pitting potential. J. Appl. Electrochem. 1990;20(6):996-999.
9. Popova A, Christov M, Raicheva S, Sokolova E. Adsorption and inhibitive properties of benzimidazole derivatives in acid mild steel corrosion. Corros. Sci. 2004;46(6):1333-1350.
10. Tang L, Li X, Li L, Mu G, Liu G. Interfacial behavior of 4- (2-pyridylazo) resorcin between steel and hydrochloric acid. Surf. Coat. Technol. 2006;201(1-2):384-388.
11. Li X, Deng S, Mu G, Fu H, Yang F. Inhibition effect of nonionic surfactant on the corrosion of cold rolled steel in hydrochloric acid. Corros. Sci. 2008;50(2):420-430.
12. Saliyan RV, Adhikari AV. Quinolin-5-ylmethylene-3-{[8-(trifluoromethyl) quinolin-4-yl] thio} propanohydrazine as an effective inhibitor of mild steel corrosion in HCl solution. Corros. Sci. 2008;50(1):55-61.
13. Sankarapapavinasam S, Pushpanaden F, Ahmed MF. Piperidine, piperidones and tetrahydrothiopyrones as inhibitors for the corrosion of copper in H_2SO_4. Corros. Sci. 1991;32(2):193-203.
14. Granese SL. Study of the inhibitory action of nitrogen containing compounds. Corros. NACE. 1988;44(6):322-327.
15. Hukovic MM, Grubac Z, Stupnisek- Lisac E. Organic corrosion inhibitors for aluminium in Perchloric acid. Corros. NACE. 1994;50(2):146-151.
16. Mahmoud SS, El-Mahdy GA. Role of Imidazolone Derivatives in corrosion inhibition of pure aluminium in hydrochloric acid solution. Corros. NACE. 1997;53(6):437- 439.
17. Desai MN, Thakar BC, Chhaya PM, Gandhi MH. Inhibition of corrosion of aluminium-51 S in hydrochloric acid solutions. Corros. Sci. 1976;16(1):9-24.
18. Rozenfeld JL. Corrosion inhibitors, Mc Graw-Hill: New York; 1981.
19. Granese SL, Rosales BM. Proceedings of the seventh European Symposium on Corrosion inhibitor: University of Ferrara, Italy; 1990.

20. Issa IM, Moussa MNH, Ghandour MAA. A study of the effect of some carboxyl compounds on the corrosion of aluminium in hydrochloric acid solution. Corros. Sci. 1973;13(10):791-726.
21. Moussa MNH, Taha FIM, Gouda MMA, Singab GM. The effect of some hydrazine derivatives on the corrosion of Al in HCl solution. Corros. Sci. 1973;16(6):379-385.
22. El-Awady YA, Ahmed AI. Effect of temperature and inhibitors on the corrosion of aluminium in 2N HCl solution, a kinetic study. J. Ind. Chem. 1985;24 A:601-607.
23. Maayta AK, Al-Rawashdeh NAF. Inhibition of acidic corrosion of pure aluminium by some organic compounds. Corros. Sci. 2004;46(5):1129-1140.
24. Popova A, Christov M, Raicheva S, Sokolova E. AC and DC study of the temperature effect on mild steel corrosion in acid media in the presence of benzimidazole derivatives. Corros. Sci. 2003;45(1):33-58.
25. Li Y, Zhao P, Liang Q, Hou B. Berberine as natural source inhibitor for mild steel in 1M H_2SO_4. Appl. Surf. Sci. 2005;252(5):1245-1253.
26. El-Naggar MM. Corrosion inhibition of mild steel in acidic medium by some sulfa drugs compounds. Corros. Sci. 2007;49(5):2226-2236.
27. Ju H, Li Y. Nicotinic acid as a nontoxic corrosion inhibitor for hot dipped Zn and Zn-Al alloy coatings on steels in diluted hydrochloric acid. Corros. Sci. 2007;49(11):4185-4201.
28. Abdallah M. Antibacterial drugs as corrosion inhibitors for corrosion of aluminium in hydrochloric solution. Corros. Sci. 2004;46(8):1981-1996.
29. Okafor PC, Ebenso EE, Epke UJ. Inhibition of the acid corrosion of aluminium by some derivatives of thiosemicarbazone. Bull. Chem. Soc. Ethiop. 2004;18(2):181-192.
30. Okafor PC, Epke UJ, Ebenso EE, Umoren EM, Leizou KE. Inhibition of mild steel corrosion in acidic medium using Allium Sativum extracts. Bull. Electrochem. 2005;21(8):347-352.
31. Umoren SA, Ebenso EE. The synergistic effect of polyacrylamide and iodide ions on the corrosion inhibition of mild steel in H_2SO_4.Mater. Chem. Phys. 2007;106(2-3):387-393.
32. El-Etre AY. Inhibition of acid corrosion of aluminium using vanillin. Corros. Sci. 2001;43(6):1031-1039.
33. El-Etre AY. Inhibition of aluminium corrosion using Opuntia extract. Corros. Sci. 2003;45(11):2485-2495.
34. Larabi L, Benali O, Mekelleche SM, Harek Y. 2-Mercapto-1-methylimidazole as corrosion inhibitor for copper in hydrochloric acid. Appl. Surf. Sci. 2006;253(3):1371-1378.
35. Lebrini M, Bentiss F, Vezin H, Lagrenée M. The inhibition of mild steel corrosion in acidic solutions by 2, 5 - bis (4-pyridyl)-1, 3, 4- thiadiazole: structure-activity correlation. Corros. Sci. 2006;48(5):1279-1291.
36. Oguzie EE, Okolue BN, Ebenso EE, Onuaba GN, Onuchukwu AI. Evaluation of the inhibitory effect of methylene blue dye on the corrosion of aluminium in hydrochloric acid. Mater. Chem. Phys. 2004;87(2-3):394-401.
37. Szklarska- Smialowska Z, Mankowski I. Crevice corrosion of stainless steels in sodium chloride solution. Corros. Sci. 1978;18(11):953-960.
38. Hosseini M, Merters SFL, Ghorbani M, Arshadi MR. Asymmetrical Schiff bases as inhibitors of mild steel corrosion in sulphuric acid media. Mater. Chem. Phys. 2003;78(4):800-808.
39. Villamil RFV, Corio P, Aghostinho SML, Rubim JC. Effect of sodium dodecylsulfate on copper corrosion in sulfuric acid medium in the absence and presence of benzotriazole. Journal of Electroanalytical Chemistry. 1999;472(2):112-119

40. Fouda AS, Moussa MN, Taha FI, Elneanaa AI. The role of some thiosemicarbazide derivatives in the corrosion inhibition of aluminium in hydrochloric acid. Corros. Sci. 1986;26(9):719-726.
41. Obot IB, Obi-Egbedi NO. Inhibitory effect and adsorption characteristics of 2, 3 - Diaminonaphtalene at Aluminium/Hydrochloric acid interface: Experimental and theoretical study. Surf. Rev. & Lett. 2008;15(6):903-910.
42. Putilova IN, Balezin SA, Baranik VP. Metallic Corrosion Inhibition, Pergamon Press: New York; 1960.
43. Dehri I, Ozcan M. The effect of temperature on the corrosion of mild steel in acidic media in the presence of some sulphur containing organic compounds. Mater. Chem. Phys. 2006;98(2-3):316-323.
44. Umoren SA, Obot IB, Apkabio LE, Etuk SE. Adsorption and corrosive inhibitive properties of Vigna unguiculata in alkaline and acidic media. Pigment & Resin Technology. 2008;37(2):98-105.
45. Noor AE. Potential of aqueous extract of Hibiscus Sabdariffa leaves for inhibiting the corrosion of aluminium in alkaline solutions. J. Appl. Electrochem. 2009;39(9):1465 – 1475.
46. Natishan PM, McCafferty E, Hubber, GK. The effect of pH of Zero charge on the pitting potential. J. Electrochem. Soc. 1986;133(5):1061-1062.
47. Luo H, Guan YC, Han KN. Corrosion Inhibition of mild steel by aniline and Alkylamines in acidic solutions. Corrosion. 1998;54(9):721-731.
48. Tang L, Mu G, Liu G. The effect of neutral red on the corrosion inhibition of cold rolled steel in 1.0 M hydrochloric acid. Corros. Sci. 2003;45(10):2251-2262.
49. Yurt A, Ulutas S, Dal H. Electrochemical and theoretical investigation of the corrosion of aluminium in acidic solution containing some Schiff bases. Appl. Surf. Sci. 2006;253(2):919-925.

Peer-review history:
The peer review history for this paper can be accessed here:
http://www.sciencedomain.org/review-history.php?iid=162&id=7&aid=748.